Construction and Building Materials, 137 (2017) 246–260

Experimental Assessment and Constitutive Modelling of Rubberised Concrete Materials

D.V. Bompa, A.Y. Elghazouli, B. Xu, P.J. Stafford, A.M. Ruiz-Teran
Department of Civil and Environmental Engineering, Imperial College London, UK

Abstract

This paper focuses on examining the uniaxial behaviour of concrete materials incorporating rubber particles, obtained from recycled end-of-life tyres, as a replacement for mineral aggregates. A detailed account of a set of material tests on rubberised concrete cylindrical samples, in which fine and coarse mineral aggregates are replaced in equal volumes by rubber particles with various sizes, is presented. The experimental results carried out in this investigation, combined with detailed examination of data available from previous tests on rubberised concrete materials, show that the rubber particles influence the mechanical properties as a function of the quantity and type of the mineral aggregates replaced. Experimental evaluation of the complete stress-strain response depicts reductions in compressive strength, elastic modulus, and crushing strain, with the change in rubber content. Enhancement is also observed in the energy released during crushing as well as in the lateral strain at crushing, primarily due to the intrinsic deformability of the interfacial clamping of rubber particles which leads to higher lateral dilation of the material. The test results and observations enable the definition of a series of expressions to estimate the mechanical properties of rubberised concrete materials. An analytical model is also proposed for the detailed assessment of the complete stress-strain response as a function of the volumetric rubber ratio. Validations performed against the material tests carried out in this study, as well as those from previous investigations on rubberised concrete materials, show that the proposed models offer reliable predictions of the mechanical properties including the full axial and lateral stress-strain response of concrete materials incorporating rubber particles.

*Corresponding Author:
Prof. A. Y. Elghazouli, Dept of Civil & Environmental Engineering, Imperial College London, UK.
Email: a.elghazouli@imperial.ac.uk

1. Introduction

Construction materials in which cementitious mixes are modified by the addition or replacement of various constituents have been constantly sought due to both performance and environmental considerations. Amongst many core targets for sustainability, the reduction of waste materials by recycling is one of the main tasks set by international organisations. Disposal of end-of-life tyres is a major environmental concern since its ineffective management can lead to undesirable consequences such as uncontrollable fires or sanitary hazards. Existing solutions involving the re-use of tyre constituents, namely rubber and steel fibres, include applications in energy production and in the landfill. Amongst existing alternatives, recycling waste tyres to produce novel concrete materials is an attractive option that could potentially combine environmental and performance advantages. As a result, in recent years, several investigations have been conducted to assess the feasibility of using recycled rubber materials in concrete.

Material tests on both fresh and hardened concrete indicated that the replacement of mineral aggregates with rubber particles modifies significantly the mechanical properties of the new composite material [1-5]. On the one hand, concrete is an implicitly brittle material which is a function of the strength of the cement paste, whereas rubber is a hyper-elastic incompressible material with high Poisson ratio and has a high tensile strength. The combination of the two results in a novel material benefitting from the strength of the concrete matrix, which governs the elastic constitutive behaviour, and the energy absorption properties of rubber.

Apart from the reduction in the unit weight of concrete due to the relatively low specific gravity of rubber [6], the replacement of mineral aggregates with rubber also results in a decrease in compression strength, splitting tensile strength and elastic modulus [7]. The strength loss due to the replacement of mineral aggregates with rubber crumb has been reported in some studies [8-10] to be related to the relatively poor bonding between the rubber and the cement. Microstructural investigations on rubberised concrete, however, support the view that the strength reduction is primarily related to the soft aggregate behaviour of the rubber particles more than due to the reduction in bond [11].

Previous studies have shown that the modification of mechanical properties is mainly a function of the grain size and percentage of rubber replacement [12, 13], and rubber treatment [14], while the rubber type only has a marginal effect [15]. Moreover, Fattuhi and Clark [15] reported that concrete containing rubber with fine grading has lower compressive strength than that containing rubber with coarse grading. For the same rubber particle content of coarse aggregate, the reduction rate of high-strength concrete was also found to be greater than that of low-strength

concrete [6]. In addition, the reduction in mechanical properties was shown to be more significant when coarse aggregate rather than sand is replaced by rubber [8].

Rubberised concrete mixtures exhibit lower compressive and splitting tensile strength, and hence reduced elastic energy in comparison with normal concrete [16]. However, they typically demonstrate a much more ductile post-peak behaviour that has the ability to absorb a relatively large amount of plastic energy under compressive and tensile loads [8]. Tyre rubber particles also provide other energy consumption mechanisms in concrete such as particle pull-out and rubber internal cracking that do not exist in normal concrete [11]. They reduce the stress singularity at the first crack tips running into the rubber/cement–matrix interface, which slows crack kinetics and delays macro-crack localisation [17]. As a result, the flexural post-cracking behaviour of rubberised concrete is positively affected by the substitution of coarse aggregate with rubber particle leading to favourable energy absorption and ductility properties [17,18]. These capabilities were however reported to be reduced with significant levels of rubber particles [6]. High toughness was also shown to be attained in samples that were provided with tyre chips [9].

In addition to the above-mentioned studies, several other investigations have substantiated the impact resistance and energy dissipation capacity of rubberised concrete [8,13]. However, most current applications of rubberised concrete have been primarily for use as non-structural elements such as crash barriers [9,11,13], floor surfaces [19], cement aggregate bases under flexible pavements [20], and vibration control-applications such as sound barriers [21-23]. The inherent energy absorption capabilities of rubberised concrete, makes it an evident candidate for impact related applications [7,15]. Although the deployment of rubberised concrete in primary structural members has not been examined in the same level of detail as for non-structural applications, the potential merits offered by the material have more recently attracted some initial attention [24,25], particularly in applications in which ductility and energy dissipation are paramount such as for seismic resistance [10,26-30]. Clearly, in such situations, to achieve satisfactory structural performance, a balance has to be sought between the enhanced energy dissipation and the reduction in mechanical properties with the increase in rubber content. This would, however, necessitate a reliable quantification of the influence of the constituent rubber on the key mechanical properties of concrete, through the development of full stress-strain characterisation models. Available studies have been related to specific sets of test data and typically addressed individual mechanical properties, such as the elastic modulus and compressive strength, rather than the full constitutive relationships. For example, Eldin and Senouci [8] used an existing model that describes the reduction of concrete strength by

accounting for the effects of macro-porosity in concrete samples where rubber aggregates were treated as large voids. Besides rubber content, Ghaly and Cahill [31] proposed a model to assess a dimensionless stress reduction factor limited to aggregate replacements up to 15%, as a function of compressive strength and water-to-cement ratio. Guneiysi et al. proposed rubber content-dependent reduction factors, which were validated against concrete mixes with replacement amounts of 50% of both fine and coarse aggregates [32]. Taha et al. [11] and Khatib and Bayomy [20] proposed similar characteristic equations that quantify the reduction in strength for rubberised concrete mixes based on a regression analysis as a function of rubber content.

As noted above, a number of previous studies have proposed expressions for estimating the individual material properties of rubberised concrete, primarily compressive strength, but there is a comparative lack of information on full constitutive relationships. Most existing analytical expressions to estimate the strength degradation are validated through a limited number of concrete mixes, with similar rubber aggregate sizes and type of mineral aggregate replaced, whereas information regarding the post-peak behaviour is scarce. To obtain a detailed insight into the behaviour, this paper describes an experimental programme carried out on rubberised concrete in which fine and coarse mineral aggregates are replaced by rubber particles. Cylindrical samples with up to 60% rubber replacement are tested under uniaxial compression to assess the complete stress-strain response, including the post-peak behaviour. Additionally, compression tests on cubic samples, and splitting tests on cylindrical specimens are carried out on compressive and tensile strengths, respectively. The test results and observations permit the definition of a series of prediction expressions for the target mechanical properties of rubberised concrete for structural design purposes as well as an analytical model for the detailed characterisation of uniaxial and lateral stress-strain response as a function of the volumetric rubber ratio. The validation of the proposed expressions for mechanical properties, undertaken against an extensive database of 238 concrete mixes including the mixes investigated in this study; demonstrate their suitability for typical design procedures. On the other hand, evaluation of the suggested uniaxial analytical model, using the test results obtained from the current investigation, illustrates its reliability for detailed assessment procedures which require the complete axial and lateral stress-strain response.

2. Experimental programme

One hundred ten (110) samples of which 60 cylindrical and 50 cubic material specimens were prepared to assess the compressive and splitting strength, as well as the full constitutive compression behaviour of rubberised concrete with various replacement ratios of both fine and coarse mineral aggregates. Following a series of trial mixes on 50 samples in which the cement type was varied whereas the remaining constituents of the mix remained unmodified, pilot tests on 4 cylindrical samples were carried out to determine the most effective testing configuration. Finally, four sets of samples (4 × Ø100×200 cylinders and 4 × 100 mm cubes for compressive tests, and 4 × Ø100×200 cylinders for splitting tests), with volumetric replacement ratios varying in the range of ρ_{vr} = *0-0.6* were tested to determine the complete stress-strain behaviour including the post-peak response. The volumetric replacement ratio ρ_{vr} is defined as the ratio between the replaced volume of mineral aggregates in the rubberised concrete and the total volume of mineral aggregates in the reference normal concrete mix.

2.1 Materials

The rubber particles used in the rubberised concrete mixes were obtained from two sources. Rubber aggregates with dimensions up to 10 mm, produced from car tyre recycling [33]. As depicted in Figure 1a, they were supplied in the following size ranges: 0-0.5 mm, 0.5-0.8 mm, 1.0-2.5 mm, 2-4 mm and 4-10 mm, and were used in the concrete mix in the 5%, 5%, 15%, 20% and 10% ratio of the total added rubber content, respectively, with remaining 45% being comprised of particles with sizes in the range 10-20 mm. The larger rubber particles were produced from truck or bus tyre recycling, with typically higher density than car tyre particles [34]. This portion was identified following a study of the workability of rubberized concrete within a wider European research project [35-38]. These proportions resulted from a detailed study on 40 mixes carried out by Raffoul et al. [38] in which the best balance between workability and strength loss was sought. All rubber particles are reported to have 25% content of carbon black, polymers in the range of 40-55%, whereas the remaining constituents are softeners and fillers. The specific gravity of rubber was 1.1, whereas the water absorption 7.1% for 4-10 mm particles and 1.05 for 10-20 mm particles.

Sand and gravel aggregates shown in Figure 1a, from naturally occurring rock deposits consisting of combinations of various minerals [39], were used for the concrete mix shown in Figure 1b. The fine aggregates with sizes up to 5 mm had a specific gravity of 2.65 and a moisture content of 5%, whereas the coarse aggregate (5-10 mm) had a specific gravity of 2.65

and a moisture content of 3%. The particle size distribution of mineral aggregates and rubber particles was determined following EN 933-1:2012 [40] as illustrated in Figure 2. In the trial mixes, CEM I 52.5N [41] and CEM II 32.5N were used to assess their influence on the compressive concrete strength at 7 and 28 days. However, in the tests used for the assessment of the constitutive behaviour, the higher strength cement was used.

2.2 Mix designs and specimen details

A reference normal concrete mix with target compressive strength of 60 MPa, typically used in bridge piers as provided by an industrial partner of the project [35] based on practical experience, was prepared the following mix ratios. This included also the amount of admixtures that they use in practice. The normal concrete (NC) reference mix had 425 kg/m^3 of cement, 820 kg/m^3 of sand, 1001 kg/m^3 of gravel, 149 litres of tap water, with 2.5 l/m^3 of plasticiser [42] and 5.1 l/m^3 of superplasticiser [43]. In the rubberised concrete mixes, 20% of the cement was replaced in equal quantities with EN 450-1 [44] fineness category S fly ash and Grade 940 silica fume [45]. They were primarily added to improve workability, segregation and slump, and to optimise the particle packing of the mixture. Rubberised concrete mixes with 20%, 40% and 60% rubber replacement by volume of mineral aggregates were produced to assess the full constitutive characteristics of rubberised concrete. The rubber quantities used in the mixes were 110 kg/m^3, 220 kg/m^3 and 330 kg/m^3, respectively. The rationale behind the mix design reported in this paper and used throughout the above-mentioned European research project was to develop an environmentally friendly concrete, primarily provided with high deformability capacities even for significant strength losses which are recovered by external confinement. This was achieved with replacement ratios of 60% of both fine and coarse aggregates using the rubber particle sizes reported in this paper and 2-4 layers of AFRP jacket confinement for applications in bridge piers and/or base isolation systems

Based on the mix optimisation study carried out by Raffoul et. al [38], which was used as a basis for the mix ratios above, it was observed that the compressive strength is slightly more influenced by coarse rubber properties, while the fine rubber was slightly more detrimental to the concrete fresh properties. The mixes without silica fume and fly ash showed poorer workability and strength. Silica fume and fly ash improved the strength and flowability with 42% and 20%, respectively, for a mix with 40% replacement of fine aggregates. The same study [38] showed that reduction of superplasticiser content by 40% reduced the flow (by up to 16%) and, more importantly, led to a reduction in mix segregation.

A rotary mixing machine with the capacity of 40 litres was mainly used for the mixes reported herein. Initially, the mineral aggregates, rubber mix and binders were mixed separately in containers. All mineral aggregates and half of the water were mixed together in the mixer for 1 minute. The rubber was then added to the mixer and mixed with the mineral aggregates and half of the water for another 1 minute. In the following phase, the binders, and the remaining water including the admixtures were mixed all together for a minimum of 3 further minutes. Supplementary plasticiser was added where the observed workability was below acceptable levels. All materials were mixed for another 2 minutes and placed afterwards in formworks, and subsequently compacted using a vibrating table until the air content in the fresh concrete was at a minimum. Although the mixing procedure may influence the performance, for the mixes reported here, the mixing procedure was maintained throughout the experimental programme, hence no considerable differences were observed.

Codified provisions allow compressive material testing primarily on cylinder samples, and also on cube specimens with specific sizes [46, 47]. In this investigation, preliminary tests were carried out at 7 days, yet the fundamental observations from tests are made at 28 days from compression tests on 100 mm × 200 mm cylinders, 100 mm cubes and splitting tests on cylinders with 100 and 102 mm diameter. The samples were cast directly in the size required in steel or plastic formworks and covered with plastic sheets until de-moulding. Two days after casting, the samples were placed in a water tank located in a curing room to ensure appropriate concrete hydration.

The ends of cylindrical samples were finished with a grinding machine on the day before the test. The cylindrical rubberised concrete samples were capped with high strength mortar and further polished with sand paper to ensure flatness of the surfaces and good contact conditions with the loading machine. The dimensions of all samples were measured to assess stress/strength and strain characteristics as a function of the recorded force and displacement. The longitudinal dimensions of the cylindrical samples and their diameters were determined as the average of a minimum of three measurements at different locations. The average dimensions of cubic samples were assessed from two measurements for each orthogonal direction.

2.2 Testing arrangement

The cylindrical specimens, used in the pilot tests and for assessing the full constitutive behaviour, were tested in a stiff four-post Instron Satec 3500 kN machine. These tests were carried out in displacement control with a compressive displacement rate of 0.1 mm/min [47, 48]. As illustrated in Figure 3a, the samples were placed on the bottom platform of the testing

machine. Loading plates of high strength steel with a diameter of 100 mm were also added at both ends of the sample. The bottom plate, depicted in Figure 3b, was a stiff 50 mm thick steel element, whereas the top plate incorporated a 3D hinge with total thickness of 75 mm. Intermediate, 'sandwich', high strength steel plates were added between the testing machine and bearing pads to allow the recording of compressive displacements in the post-peak regime.

For all cylindrical specimens tested in compression, the sample pre-peak axial behaviour was recorded using three displacement transducers attached to two steel rings positioned symmetrically around the central cross-section at a gauge length of 100 mm (Figure 3b). Each steel ring was connected directly to the sample through three steel bolts in order to avoid interaction with the specimen. Two other independent transducers were placed between the two sandwich plates to record the axial deformation in the post-peak regime. Test measurements were averaged and transformed into strains by using the measured gauge length for each sample. The two measurement systems were required in order to assess the complete constitutive characteristics since, in the pre-peak range, the behaviour is governed by stable deformations, whereas in the post-peak regime the axial deformations are governed by macro-cracking which may lead to unstable measurements from the ring transducers [48, 49]. Lateral deformations were recorded by four transducers attached to the central steel ring located at the middle of the specimen, as illustrated in Figure 3b, and averaged to assess the constitutive behaviour.

On the other hand, compressive tests on cubes as shown in Figure 4a and splitting tests on cylinders as shown in Figure 4b, were carried out in force control using a 3000 kN Automax machine. The loading rate was 0.3 MPa/sec [47] and 0.01 MPa/sec [50] for the two types of tests, respectively. The force control testing machine had a top plate provided with a hinge to accommodate rotations from a potential non-symmetrical behaviour of the samples. The splitting tests were carried out in an existing testing rig positioned between the machine loading plates, specifically designed for this purpose.

2.3 Mechanical properties of rubberised concrete

2.3.1 Pilot tests

The vibration of rubberised concrete may lead to agglomeration of rubber particles at the top of the sample. Under compressive testing, this may lead to end failure of the sample which is a characteristic of the specimen, rather than the material. An analysis of sample halves obtained from initial splitting tests (Figure 4b) using digital image processing techniques for examining

aggregate distribution along their longitudinal cross-section show that the rubber had the tendency to lift during vibration of fresh concrete which leads to a zone of agglomeration of rubber particles at the top of the sample (Figure 5a). This created a weaker region, in which the strength of the material is governed by the rubber. For such cases, the end confinement is instrumental to translate the failure outside of this region. Although this effect was observed in some pilot material test samples, in large structural members recently tested by the authors [30], using rubberised concrete with 60% replacement of both fine and coarse aggregates and provided with longitudinal and transverse reinforcement, the exterior surface had a good appearance with no observed sign of segregation. In the structural members, use was made of vibrators provided with pokers after the concrete was poured in several layers to obtain the highest level of homogeneity possible. This technique may result in a better homogenization of the mix in comparison with the use of vibrating tables.

A series of pilot tests were carried out in which jubilee clips at the sample ends were used to overcome potential end failures. Additionally, a low friction bearing systems by means of polytetrafluoroethylene (PFTE) sheets [48], placed between the sample and loading plates, were used and compared with typical testing configurations without PFTE. Figure 5b depicts a comparison between four samples made of rubberised concrete with replacement ratio of ρ_{vr} = 0.6 as follows: (i) R60-00 without jubilee clips and with high friction loading system (i.e. direct contact between loading plates and sample); (ii) R60-J0 with jubilee clips and with high friction bearing system; (iii) R60-0P without jubilee clips and with low friction bearing system; and (iv) R60-JP with jubilee clips and with low friction bearing system.

As observed in Figure 5b, all cylindrical samples from the pilot tests had similar stiffness, strength and post-peak behaviour. Table 1 shows that the variance between recorded strengths f_{cr} and the dissipated energy G_c after crushing is minimal. On the other hand, the elastic stiffness E_{cr} and crushing strain ε_{cr1} show some scatter, yet within reasonable limits for such material. Close examination of the failure pattern depicted in Figure 5c shows that members without jubilee clips developed end failures, whereas others had sliding failures which are typically expected for concrete specimens. This indicates that in cylindrical samples made of concrete with significant rubber content, end confinement combined with ground and capped loading surfaces are required to achieve expected failure modes under compression. Additionally, the use of low friction bearing systems had a minor influence on the stress-strain characteristics and failure mode. Consequently, the pilot tests suggested the suitability of test set-ups in which samples are provided with end confinement and connected directly to the loading plates.

2.3.2 Stress-strain response

Material characterisation tests on rubberised concrete and normal concrete cylinders were carried out to assess the influence of rubber content on the constitutive behaviour. The investigated rubber replacement ratios were 20%, 40% and 60% of the total aggregate volume, as described previously in this section. Figures 6a-d depict three axial and lateral stress-strain recorded test curves and their average. The stress-strain curves include both pre-peak and post-peak behaviour as recorded in the tests. The post-peak response is plotted down to 30% of the compressive strength f_{cr}. Beyond this value, an approximate response band is plotted with reference to the negative stiffness of the descending branch.

The comparative assessment of σ-ε curves from Figures 6a-d shows clear reductions in strength and stiffness with the increase of rubber content. The strength is approximately halved with each 20% increment increase of aggregate replacement. The compressive strength of concrete f_{cr} with ρ_{vr} = 0.6 (R60) is about 10% of the normal concrete R00. The elastic modulus E_c is also significantly affected with R60 exhibiting 20% of the modulus from R00. On the other hand, the reduction in the crushing axial strain ε_{cr1} is comparatively less with about 40% reduction from R00 to R60. A stronger influence on mechanical properties is typically observed for small replacement ratios and tends to stabilise as the rubber content increases.

Beyond the peak, the stiffness response in the lateral direction, governed by the sliding behaviour of the two bodies separated by the macro-crack, flattens with the increase of rubber replacement. In addition to the interlock of mineral aggregates, this is produced by the intrinsic deformability of the interfacial clamping rubber particles which enable higher dilation of the sample at lower sliding displacements. In contrast to the average test measurements for normal concrete, in which a distinct peak lateral strain is observed as the rubber content increases, the peak lateral strain takes the form of a plateau, rather than a discrete point. On the other hand, the post-peak axial compression behaviour exhibits increased softening with the decrease in strength. Tests showed softer post-crushing behaviour which typically leads to similar or higher energy dissipation in the post-peak regime.

The pre-peak behaviour of the concrete tests was strongly influenced by the rubber replacement of the mineral aggregates. As illustrated in Figure 6, elastic stiffness E_{cr} degraded with the increase in rubber content. Naturally, the rubber aggregates are softer and lighter in weight compared to mineral aggregates. In this case, the matrix, comprised of binders, water and admixtures, is much stronger than the rubber aggregates but may be weaker than the mineral

aggregates. Hence, for the rubberised concrete materials, the reduction in stiffness is a function of the stiffness ratio between the cement matrix and inclusions (rubber particles and voids). Around the peak, the tangent modulus decreases to zero and crushing occurs, which is generally triggered by de-bonding of the aggregates from the cement paste. As the bond capacity of rubber particles is lower than that of mineral aggregates, this effect is activated at earlier stages [10]. Tensile cracks therefore typically occur around the crack which eventually produces visible macro-cracks. At the peak, the macro-crack, in the form of the sliding crack, governs the behaviour and results in significant lateral expansion and volume increase even with an increase in axial compaction.

2.3.3 Influence of rubber content on the mechanical properties

As depicted in Figures 7a-c and Table 2, similarly to the stiffness E_{cr} degradation with rubber content as described above, test measurements of compressive strength f_{cr} and axial strain at crushing ε_{cr1} showed similar decreasing trends. For the concrete samples without rubber, the average $E_{cr,R00}$ = 42.3 GPa, $f_{cr,R00}$ = 70.2 GPa and the corresponding average $\varepsilon_{cr1,R00}$ = 0.228 %. The average E_{cr} for samples with rubber was 19.6 GPa, 14.1 GPa and 9.03 GPa for R20, R40 and R60, respectively. The recorded f_{cr} and ε_{cr1} were 29.7 MPa and 2.13% for 20% replaced mineral aggregates, 13.3 MPa and 1.38% for 40% replacement, and 7.06 MPa and 1.37% for the material with the highest rubber content (60%). Although an evident decrease was recorded for axial compaction, the lateral dilation in Figure 7d exhibited a rather constant average response for the rubberised concrete samples with lateral strains ε_{cr2} that varied between 1.20% - 1.30%. In the post-peak response, the shape of the descending branch showed flatter inclination and the ultimate recorded strain increased (at 30% of $f_{cr,Rij}$) as the rubber content increased.

In addition to the cylindrical samples used for the stress-strain assessments, 100 mm cubes were tested in compression and cylinders with 100 mm diameter were subjected to splitting (Figure 4a,b). This enables a direct comparison of the compressive strength loss as a function of sample type (Figure 7b) and provides information on the tensile strength of rubberised concrete (Figure 7e). Material strengths assessed on cubes are higher than the corresponding cases on cylinders. Smaller cylinder-to-cube strength ratios are obtained for rubberised concrete in comparison with typical cases of normal concrete (about 0.8 for normal strength concrete). The average cylinder-to-cube test strength $f_{cr}/f_{cr,cube}$ is 0.91, 0.58, 0.54 and 0.59 for 0%, 20%, 40% and 60% replacement, respectively. The splitting strength decreases nearly in proportion to the rubber content from 4.99 MPa for normal concrete to 1.20 for rubberised concrete with the highest amount of rubber content.

The curve in the top left corner of Figure 7f describes the post-peak stress decrease with the increase of crushing crack displacement w_{cr} up to the test recorded residual value of $0.3f_{cr}$ and the corresponding $w_{cr,test}$. The area below the curve is referred to as the crushing energy G_c and may be defined as the energy dissipated during crushing. Based on this assumption, the test recorded stress-strain curves were analysed and the energy released during crushing was assessed. The samples with the lowest amount of rubber (ρ_{vr} = 0.2) seem to be governed by a rather brittle response in comparison to those with ρ_{vr} = 0.4-0.6. For ρ_{vr} = 0.2, the concrete seems to govern the post-crushing behaviour since the assessed energy G_c is smaller than the assessed crushing energy for R00. As shown in Figure 7f, for the cases with 40% and 60% replacement, the released energy increases and a more ductile response is observed, with the rubber having a significant influence on the behaviour.

The material tests described in this section on cylinders and cubes (Figure 8) allowed direct assessment of the complete compressive constitutive behaviour of concrete materials with embedded rubber particles. Additional considerations regarding the strength degradation both in compression and tension were given as well as an evaluation of the energy released during crushing. Key observations from the resulting stress-strain and failure characteristics described above are further used in the following section for proposing relationships for predicting the mechanical properties of rubberised concrete material as a function of the rubber content.

3. Prediction of mechanical properties

In addition to the experimental results presented in Section 2 on the three rubberized concrete mixes and the reference normal concrete mix, the prediction equations proposed in this section incorporate an extensive database of other 238 concrete mixes of which 198 embed rubber particles and 40 corresponding reference ones [1, 6-12, 16-20, 32, 38, 51-56]. Thus, the entire database includes average mechanical properties from 238 concrete mixes, each determined from a minimum of three material tests, which leads to a total of over 714 samples. Expressions to assess the compressive strength, tensile strength and modulus of elasticity are proposed herein, followed in the subsequent section by suggested representations for the complete constitutive behaviour of rubberised concrete materials.

3.1 Compressive strength

The compressive strength assessments for mixes reported in the database and Table 3 were carried out on both cylinders of 100 mm × 200 mm and 150 mm × 300 mm dimensions, as well

as on cubes of 50 mm, 100 mm or 150 mm sizes. Fattuhi and Clark [15] noted however that it is difficult to make an accurate comparison between the results of various investigations on rubberised concrete since the shape and size of specimens influence the compressive strength of concrete, which is also the case for normal concrete. Due to specimen geometry, the volumetric expansion of cylinders is distinctive of a cube made of the same material resulting in dissimilar failure patterns and consequently different nominal strength.

Several previous studies dealt with size effects in concrete material testing. For example, Neville [57] proposed conversion factors to account for the size effect in compression based on the volumetric dimensions of the samples. Mansur and Islam [58] and Yi et al. [59] used regression analyses to obtain correlation functions between various sample sizes and shapes. Nielsen and Hoang [60] reported that size effects in concrete can be described by a Weibull distribution, in which the reference sample is characterized by its strength $f_{cr,ref}$ and volume $V_{cr,ref,}$ and the element that requires conversion is defined by the strength $f_{cr(d)}$ and volume $V_{cr(d)}$, related through Equation (1) (where m=30 for compression). To harmonize the test results in the database considered in this investigation, the compression strength results are adjusted in relation to reference cylindrical samples of 100 mm × 200 mm and a reference age of 28 days.

$$f_{cr,ref} = f_{cr(d)} \left(V_{cr(d)} / V_{cr,ref} \right)^{1/m} \quad (1)$$

Figure 9 illustrates the relationship between the compressive strength degradation (CSD) as a function of rubber replacement. On the ordinate axis, the rubberised concrete strength f_{cr} is normalised against the reference strength of the conventional concrete f_{c0}, whereas on the abscissa the rubber content is reported as volumetric ratio ρ_{vr}. The volumetric ratio ρ_{vr} is the volume of rubber that replaces the mineral aggregates regardless of its size and type. The plot includes the results of the tests described in Section 2, used as a reference, results from the database in Table 3 and the exponential trend lines for the results. Close inspection of the influence of the type of rubber on the strength degradation indicates that for replacements of only coarse mineral aggregates, the scatter between results is relatively large and the database trend line deviates from the reference tests trend line. In contrast, for replacement of fine or both fine and coarse aggregates, the trends are nearly identical.

The strength of concrete is typically influenced by the cement type, water-cement ratio, mineral aggregate type, source and size, the presence of admixtures (e.g. plasticisers, retarders), the presence of other cementitious materials (e.g. fly ash, micro-silica, metakaolin). Additionally, for rubberised concrete mixes, the rubber type, size and replacement proportions also have a

significant influence on the achieved strength. A detailed examination of the results from Section 2, as well as from the database, show that the main parameters governing the strength of rubberised concrete are the volumetric replacement ratio, the size of replaced aggregate and characteristics of rubber particles. It was also observed that strength degradation can be affected by the testing arrangement, control and instrumentation, which increases the uncertainty in modelling.

Close inspection of the database indicates that the rubber and mineral aggregate sizes have a relatively insignificant influence on strength degradation. In contrast, the volumetric rubber ratio ρ_{vr} strongly affects the compressive strength, while the type of mineral aggregate replaced also has an influence. The results for the coarse aggregate replacement also indicate a comparatively greater level of dispersion. On the other hand, no clear trend exists with regard to the influence of the aggregate size factor.

To represent the compressive strength degradation (CSD) for practical application, a parametric equation was developed. The functional form for this model was empirically motivated and is shown in Equation (2). The function passes through (ρ_{vr}, f_{c0}/f_{cr}) = 0,1, and captures the rapid reduction in strength shown by the data. The volumetric rubber ratio ρ_{vr} and the type of replaced aggregate are incorporated in the formulation. The latter is represented by a factor λ which accounts for the size range of the mineral aggregate replaced; i.e. fine (FA), coarse (CA) or coarse and fine (CA+FA). The values for λ were inferred from the database after classifying the data into bins according to the replaced aggregate size. The λ factor was chosen separately for each type of aggregate replaced in order to obtain the best estimates for f_{cr}. Considering the 238 mixes from the database (Table 3), which also includes the test results from the current investigation and described in Section 2, Equation (2a) may be used for assessments of f_{cr}. As shown in (Equation 2b), $\lambda = 2.43$ for fine mineral aggregate (FA) replacement, $\lambda = 2.90$ for both fine and coarse aggregates (CA+FA) replacement, and $\lambda = 2.08$ if rubber replaces coarse aggregates (CA).

$$f_{cr} = \frac{1}{1+2\left(\frac{3\lambda\rho_{vr}}{2}\right)^{3/2}} f_{c0} \tag{2a}$$

where λ is function of the replaced mineral aggregate size

$$\lambda = \begin{cases} 2.43 \rightarrow d_{g,repl} \in (0,5) \\ 2.90 \rightarrow d_{g,repl} \in (0, d_{g,max}) \\ 2.08 \rightarrow d_{g,repl} \in (5, d_{g,max}) \end{cases} \quad (2b)$$

The database in the Table 3 contains rubberised concrete mixes with volumetric replacement factors ρ_{vr} up to 0.65. It is approximately equivalent to total replacement of the fine and coarse aggregates or 60% replacement of the fine and coarse aggregates. There is very limited data on mixes in which $\rho_{vr} > 0.6$, primarily since above this limit the physical characteristics are strongly governed by the rubber and because of the concrete workability and slump decrease drastically [38]. The strength results used for validation of Equation (2) are average strengths on a minimum of three samples, as reported in the literature. Hence, the analytical model is validated using a minimum of 714 tests, which involve a wide range of material variations, as follows:

- Fine mineral aggregate replacement by mass up to 100% (average=14.62%)
- Coarse mineral aggregate replacement by mass up to 100% (average=16.27%)
- Total mineral aggregate replacement by total aggregate volume up to 64.8% (average=16.03%)
- Average rubber size $d_{r,avg}$=1.05-27.5 (average = 12.6)
- Maximum rubber aggregate size $d_{r,max}$ = 50 mm
- Maximum mineral aggregate size $d_{g,max}$ = 10 - 40 mm
- Volumetric replacement factor ρ_{vr} = 0.015 - 0.648
- Reference concrete compressive strength f_{c0} = 12.70 – 97.2 MPa

The results from the database and the reference results from Section 2 are plotted against average exponential trend lines and the proposed Equation (2a) accounting for λ factors from Equation (2b) in Figure 9. Table 3 depicts the main characteristics of the mixes used for the calibration of Equation (2). For a target total average test-to-predicted strength ratio of 1.00, the coefficient of variation (COV) increases from 10.1% for CA+FA to 12.1% for FA and to 13.4% for CA. Although the COV for each group of mixes is rather small in the majority of the cases, low average test-to-predicted values are obtained particularly for the case of replacement with coarse aggregates CA (Table 3). Predictions for rubberised concrete materials in which fine aggregates (FA, CA+FA) are replaced show a more uniform response, both in terms of individual average and COV. Additionally, as observed in Figure 9 and Table 3, combined

aggregate replacements may lead to an optimal mix and a more stabilised compressive behaviour in comparison with cases with only fine or only coarse aggregates replaced.

As noted before, testing arrangements may also have an influence on the mechanical characteristics. For controlled set-ups in which displacement control is combined with detailed instrumentations, the predicted-to-test compressive strengths show an average of 1.04 and a COV of 0.08. Neville [61] and Himsworth [62] investigated the variability of concrete and its effect on mix design. They showed that higher dispersion between results is typically obtained for low concrete strengths, noting that very low COV values are attainable in well-controlled laboratory tests (~5%), and excellent results are referred to when the COV is less than 12%. The control is fair when COV is about 18% and situations of poor control are when COV values are above 25%.

Based on the database results, a relationship between the cube and cylinder strength of rubberised concrete could not be proposed since there are very few reports in which both cubes and cylinders were tested. The $f_{cr}/f_{cr,cube}$ ratios reported in Section 2.3.3 of the paper may be used as approximate conversion factors for rubberised concrete mixes that have very similar characteristics to those reported here.

3.2 Modulus of elasticity

Using the available data from the tests undertaken in this study as well as those available from the database, Equation (3) is suggested for predicting the elastic modulus of rubberised concrete as a function of the rubberised concrete compressive strength assessed by means of Equation (2).

$$E_{cr} = 12\left(\frac{f_{cr}}{10}\right)^{2/3} \tag{3}$$

Figure 10a depicts the relationship between f_{cr} and the E_{cr} obtained from tests using 110 concrete mixes and the tests described in Section 2, as well as the analytical representation of Equation (3). Figure 10b illustrates the stiffness degradation as a function of ρ_{vr}. For the validation, all tests are treated in a similar manner disregarding the type of aggregate since limited results exist for rubberised concrete materials with fine aggregate replacement. Relatively more variation is observed in comparison with the predictions for compressive strength, with an average in reported-to-predicted elastic modulus of 1.04 and an associated COV of 0.21.

3.3 Splitting strength

As above, a relationship between the splitting tensile strength $f_{ctr,sp}$ and rubberised concrete strength f_{cr} is suggested herein. The results from 89 rubberised concrete mixes from available databases and the test results from Section 2, are used in deriving Equation (4). Figure 11a illustrates the relationship between $f_{ctr,sp}$ and f_{cr}, as obtained from the test results and Equation (4). Figure 11b depicts the splitting strength $f_{ctr,sp}$ degradation as a function of ρ_{vr}. The predictions show good agreement with tests with an average test-to-predicted strength ratio of 1.01 and COV of 19%.

$$f_{ctr,sp} = 0.24\, f_{cr}^{\,2/3} \tag{4}$$

To sum up, a series of expressions to predict the compressive strength f_{cr}, modulus of elasticity E_{cr} and splitting strength $f_{ctr,sp}$ of concrete materials incorporating embedded rubber particles are proposed in this section. The analytical equations are validated against the test results described in Section 2 and an extensive database of rubberised concrete mixes with a wide range of parameter variations. The suggested expressions account for the influence of rubber content ρ_{vr} and type of mineral aggregate replaced. They offer a reliable prediction of the basic mechanical properties and enable the development of equations to assess the full constitutive behaviour of rubberised concrete materials, as discussed in the following section.

4. Complete constitutive relationships

4.1 Proposed model

Based on the test results and observations described above, this section proposes a uniaxial unconfined constitutive model for rubberised concrete materials. The model uses the equations proposed in Section 3 to estimate the elastic modulus E_{cr}, compressive strength f_{cr} and splitting tensile strength $f_{ctr,sp}$ as a function of the mechanical properties of the reference concrete without rubber (i.e. $\rho_{vr} = 0$). The crushing strain $\varepsilon_{cr1,1}$ of rubberised concrete is a function of the crushing strain of the reference concrete $\varepsilon_{c01,1}$, determined used Equation (5) [63] and ρ_{vr}. With reference to Figure 12, the uniaxial behaviour is divided into three stages: initial, degraded and post-crushing. In the initial stage, the material is defined by Equation (6) up to stress ratios below the elastic limit $\sigma/f_{cr} \leq 0.3$ (Equation 7). The second stage is defined by a second degree polynomial function, depicted by Equation (8), which is bounded by the proportionality limit $\varepsilon_{cr1,el}$ and the crushing strain $\varepsilon_{cr1,1}$ which can be determined from Equation (9). The post-crushing stage

(Equation 10) is dependent on the post-peak crushing energy ($g_{c,2}$) in Equation (11), represented by a triangular distribution (Figure 12).

$$\varepsilon_{c01,1} = 0.7 f_{c0}^{\ 0.31} \tag{5}$$

$$\frac{\sigma_{1,i}}{f_{cr}} = E_{cr}\varepsilon_1 \rightarrow \varepsilon_1 \leq \varepsilon_{cr1,el} \tag{6}$$

$$\varepsilon_{cr1,el} = 0.3 f_{cr} / E_{cr} \tag{7}$$

$$\frac{\sigma_{1,i}}{f_{cr}} = \frac{5}{3}\left(\frac{\varepsilon_1 - \varepsilon_{cr1,el}}{\varepsilon_{cr1,1}}\right) - \left(\frac{\varepsilon_1 - \varepsilon_{cr1,el}}{\varepsilon_{cr1,1}}\right)^2 + \frac{0.3 f_{cr}}{f_{cr}} \rightarrow \varepsilon_1 \in \left(\varepsilon_{cr1,el}, \varepsilon_{cr1,1}\right) \tag{8}$$

$$\varepsilon_{cr1,1} = \left(1 - \rho_{vr}\right)\varepsilon_{c01,1} \tag{9}$$

$$\frac{\sigma_{1,i}}{f_{cr}} = \frac{1}{8}\left(\frac{f_{cr}}{g_{cr,2}} - 1\right)^2 \left(\frac{\varepsilon_1 - \varepsilon_{cr1,2}}{\varepsilon_{cr1,1}}\right)^2 - \frac{6}{8}\left(\frac{f_{cr}}{g_{cr,2}} - 1\right)\left(\frac{\varepsilon_1 - \varepsilon_{cr1,2}}{\varepsilon_{cr1,1}}\right) + \frac{f_{cr,2}}{f_{cr}} \rightarrow \varepsilon_1 \geq \varepsilon_{cr,u} \tag{10a}$$

$$\text{where } \frac{f_{cr,2}}{f_{cr}} = \frac{5}{3}\left(\frac{\varepsilon_{cr1,1} - \varepsilon_{cr1,el}}{\varepsilon_{cr1,1}}\right) - \left(\frac{\varepsilon_{cr1,1} - \varepsilon_{cr1,el}}{\varepsilon_{cr1,1}}\right)^2 + \frac{0.3 f_{cr}}{f_{cr}} \tag{10b}$$

$$g_{cr,2} = \left[\left(1 + \rho_{vr}\right) f_{cr}\right]^{2/3} \tag{11}$$

The lateral strain ε_{cr2} is a function of the axial strain ε_{cr1}, stress ratio σ/f_{cr} and ρ_{vr}. It is assumed that prior to crushing the ε_{cr2} follows a bi-linear representation depicted by two regimes as a function of the volumetric rubber ratio. Assessment of lateral response requires the uniaxial σ-ε relationship (Equations 6-11) and the lateral strain at crushing $\varepsilon_{cr2,1}$. Based on results and observations from Section 2, $\varepsilon_{cr2,1}$ corresponding to the crushing strain of rubberised concrete $\varepsilon_{cr1,1}$ can be estimated by Equation (12).

Figure 13 depicts the relationship between the stress factor σ/f_{cr} and the strain ratio $\varepsilon_{cr1}/\varepsilon_{cr2}$ as obtained from the tests. It can be observed that as the rubber content increases, the curve becomes softer, in a bi-linear representation; the slope change occurs at lower axial stress levels for high rubber replacements. This shows that the lateral-to-axial deformation behaviour is strongly governed by rubber deformation. In the analytical approach, this aspect is captured by Equation (13) which may be used to estimate the axial stress ratio η at which the lateral behaviour starts to be governed by the rubber. Up to η, the lateral strain may be assessed using Equation (14), and beyond η it can be estimated through Equation (15). Beyond crushing, the lateral response of rubberised concrete is a function solely of the axial stress ratio (Equation 16). The proposed equations predict the σ-ε response in absolute values.

$$\varepsilon_{cr2,1} = \frac{4}{3\left(1-\rho_{vr}\right)}\varepsilon_{cr1,1} \tag{12}$$

$$\eta = 1 - 3{\rho_{vr}}^2 / 2 \tag{13}$$

$$\frac{\varepsilon_{cr2}}{\varepsilon_{cr1}} = \left(\frac{\sigma_{1,i}}{f_{cr}}\right)\frac{1}{3\left({\rho_{vr}}^2+1\right)} \rightarrow 0 \geq \varepsilon_{cr1} > \varepsilon_{cr1(\eta f_{cr})} \tag{14}$$

$$\frac{\varepsilon_{cr2}}{\varepsilon_{cr1}} = \left(\frac{\sigma_{1.i}}{f_{cr}}\right)\frac{4}{3\left(1-{\rho_{vr}}^3\right)} + \varepsilon_{cr2(\eta)} \rightarrow \varepsilon_{cr1(\eta f_{cr})} \geq \varepsilon_{cr1} > \varepsilon_{cr1,1} \tag{15a}$$

$$\text{where } \varepsilon_{cr2(\eta)} = \eta\frac{\varepsilon_{cr1(\eta)}}{3\left({\rho_{vr}}^2+1\right)} \tag{15b}$$

$$\frac{\varepsilon_{cr2}}{\varepsilon_{cr1}} = 10\left(1-\frac{\sigma_{2,i}}{f_{cr}}\right) \rightarrow \varepsilon_{cr1} \geq \varepsilon_{cr1,1} \tag{16}$$

Direct uniaxial tensile tests on rubberised concrete are absent, and existing information about tensile behaviour is derived from indirect splitting or flexural tensile tests. The database of tests described in Section 3, as well as tests carried out in this study, were employed to assess the splitting strength (Equation 4) of rubberised concrete as a function of the compressive rubberised concrete strength (Equation 2). Although the exact ratio between the tensile and splitting strength of rubberised concrete may differ, Equation (17a) and (17b) [64] can be further used for tensile strength assessment. The tension behaviour before cracking can be accounted for by assuming the elastic stiffness determined using Equation (3).

$$f_{ctr,sp} = 0.9\, f_{ctr} \tag{17a}$$

$$f_{ctr} = 0.21\, {f_{cr}}^{2/3} \tag{17b}$$

Limited research currently exists regarding the post-cracking response of members provided with rubber particles. The maximum crack mouth opening as directly reported in the literature, or determined by means of rigid plastic assumptions on tests reported by Liu et al. [54], Toutanji [9] and Turtansize and Garros [17] indicate values below those reported for normal concrete which vary between 160-180μm [65]. In the tests carried out by Taha [11] as well as Najim and Hall [66] on 13 mixes with replacement ratios ρ_{vr} of 0-0.65, the maximum crack displacement $w_{max,r}$ varied between 144 to 366 μm (Figure 14a), with an average of 229 μm. Accounting for a linear relationship between ρ_{vr} and $w_{max,r,}$ the latter can be estimated by Equation (18) as a function of the base maximum crack width ($w_{max,0}$*=180* μm for ρ_{vr} = 0).

$$w_{\max,r} = w_{\max,0} + 0.3\rho_{vr} \text{ (in mm)} \quad (18a)$$

$$w_{\max,0} = 0.18mm \quad (18b)$$

For simplicity, as illustrated in Figure 14b, a bi-linear tensile stress-strain diagram may be assumed. Alternatively, an exponential representation [67] can also be employed on the condition that the fitting parameters of the model are used in order to obtain the lowest bound of G_f.

4.2 Validation against test results

Figure 15 depicts the predicted compressive constitutive behaviour using Equations (5-16) against the stress-strain relationships obtained from the tests described in Section 2. The comparative assessment between predicted and experimental constitutive response shows good agreement. For the case without rubber, the crushing strain $\varepsilon_{cr1,1}$ corresponds to the crushing strain of normal concrete $\varepsilon_{c01,1}$ as determined from Equation (5) [63] since ρ_{vr} = 0. This illustrates a rather flexible response in comparison with that obtained from tests, and a lower compressive strength f_{cr} since the polynomial coefficients in Equation (10) were selected to predict a lower bound value.

For the case with low rubber content (ρ_{vr} = 0.2), the predicted response corresponds to the lower bound of σ-ε curves from tests. Although the predicted compressive strength shows the highest variance with respect to the test average, both the lateral and axial strains exhibit the best estimates in comparison with the average strain from the tests. For higher amounts of rubber (ρ_{vr} = 0.4-0.6) the predicted constitutive response is similar to that assessed from experimental results in terms of stiffness, strength and strains. Additionally, the assumptions regarding the amount of energy dissipated in the post-peak regime lead to good estimates of the descending branch for all the cases investigated.

The results from Equations (6-18) show a test-to-predicted compressive strength average of 1.04 and a COV of 6.7%, whereas the average ratio for axial crushing strains is 1.00 with a COV of 17.6%, and the average ratio between lateral strains at crushing is 1.11 with a COV of 18.5%. The predictions in Figure 15, combined with previous statistical results, show that the proposed uniaxial constitutive model may be used to assess the detailed characteristic behaviour of concrete materials incorporating rubber particles. The above-proposed model offers a reliable and practical approach, in terms of determining the target mechanical properties of rubberised concrete for analysis and design purposes, as well as for detailed assessments of axial and lateral stress-strain responses.

Figure 16 plots a comparison between the Eurocode 2 stress-strain σ-ε relationship for non-linear analysis against predicted responses for ρ_{vr}=0 and f_{c0}=50 MPa by Equations (5-11) by accounting for four cases at which Equation (10a,b) activates at a fraction of the crushing strain $\varepsilon_{c01,1.}$ It may be observed that elastic E_{cr} and secant stiffness, crushing strain $\varepsilon_{c01,1}$ and compressive strength f_{c0} show a close match with the Eurocode 2 σ-ε relationship. It is also worth noting that Equation (8) in the paper, which predicts the compressive behaviour between $0.3f_{cr}$ to $1.0f_{cr}$, also shows good agreement with the Eurocode 2 in the post-peak branch if Equation (10a,b) is activated stages beyond $\varepsilon_{c01,1}$. However, to obtain a lower bound of the crushing energy and as well as a close σ-ε response for high strength concrete (ρ_{vr}=0) in the predictions of the model from Figure 15, the activation of Equation (10a,b) begins at $\varepsilon_{c01,1}$ for normal concrete and at $\varepsilon_{cr1,1}$ for rubberised concrete.

5. Conclusions

This paper focused on examining the uniaxial behaviour of concrete materials incorporating rubber particles obtained from recycled end-of-life tyres as replacement of mineral aggregates. A detailed account of a set of 110 material tests, including experimental assessments of the complete stress-strain response of rubberised concrete carried out on cylindrical samples, was presented. The main parameter investigated in tests was the rubber replacement ratio by replacing both fine and coarse mineral aggregates in equal volumes by rubber particles with various sizes. Additionally, a detailed analysis of a database on average test results from 238 rubberised concrete mixes and their reference concrete mixes, including tests undertaken in this study, was carried out. The test results and observations described in this paper enabled the definition of a series of prediction expressions to estimate the mechanical properties of rubberised concrete materials as well as the development of an analytical model for detailed assessment of the complete stress-strain response of the material as a function of its volumetric rubber ratio. The experimental and analytical investigations in this paper, allow for the following key observations to be highlighted:

- The experimental results showed that the rubber particles influenced the mechanical properties as a direct function of the volume of the mineral aggregates replaced. Additionally, the database analysis showed that, besides the volumetric replacement ratio, the type of mineral aggregate replaced also affects the behaviour, with relatively less influence from the type and characteristics of the rubber added.

- Uniaxial compression tests, carried out on cylindrical samples to assess the complete stress-strain response, showed that the compressive strength, elastic modulus, and crushing strain decrease with the increase in rubber content. On the other hand, the lateral strain at crushing and the energy released during crushing is enhanced due to the presence of rubber.
- The tests showed that the reduction in elastic stiffness is mainly a consequence of the flexibility and light weight of rubber aggregates in comparison with mineral aggregates. The presence of rubber particles with inherently low bond capacity leads to premature crushing, in comparison with normal concrete, as a function of the rubber content. This initiates tensile cracks within the material that eventually leads to a sliding macro-crack which produces large lateral expansion and volume increase.
- Beyond peak, the stiffness response in the lateral direction, governed by the sliding behaviour of the two bodies separated by the macro-crack, flattens with the increase of rubber content due to the intrinsic deformability of the interfacial clamping rubber particles which enables higher dilation of the sample at lower sliding displacements. The experimental response typically exhibited softer post-crushing behaviour and similar or higher energy dissipated in the post-peak regime.
- The proposed expressions for estimating the mechanical properties, which have been validated using an extensive database of 198 rubberised concrete mixes, offer significant improvements for design purposes in comparison with existing analytical models. Existing strength prediction relationships have only been validated for a limited number of concrete mixes incorporating similar rubber particle sizes and types of mineral aggregate replaced.
- A novel uniaxial constitutive analytical model for rubberized concrete is proposed and validated against the test results carried out within this study. The model provides a reliable representation, which has been lacking to date, for assessing the complete axial and lateral stress-strain response for rubberized concrete.

Acknowledgements

The authors acknowledge the financial support of the European Union Seventh Framework Programme FP7/2007- 2013 under grant agreement No 603722 within the project ‘Anagennisi: Innovative Use of all Tyre Components in Concrete’ for the tests described in this paper. The discussions with collaborators within the project, particularly from the University of Sheffield, are gratefully acknowledged. The authors would also like to thank the technical staff of the Structures Laboratories at Imperial College London, particularly Mr. T. Stickland, for their assistance with the experimental work. The support of Adria Abruzzo, Hope Construction Materials, Elkem and Sika through the provided materials is gratefully acknowledged.

References

[1] Hernandez-Olivares F, Barluenga G, Bollatib M, Witoszekc B. Static and dynamic behaviour of recycled tyre rubber-filled concrete, Cement and Concrete Research 2002;32(10):1587–1596

[2] Moustafa A, ElGawady MA. Mechanical properties of high strength concrete with scrap tire rubber. Construction and Building Materials. 2015 Sep 15;93:249-56.

[3] Sgobba S, Borsa M, Molfetta M, Marano GC. Mechanical performance and medium-term degradation of rubberised concrete. Construction and Building Materials. 2015 Nov 15;98:820-31.

[4] Youssf O, Mills JE, Hassanli R. Assessment of the mechanical performance of crumb rubber concrete. Construction and Building Materials. 2016 Oct 30;125:175-83.

[5] Rezaifar O, Hasanzadeh M, Gholhaki M. Concrete made with hybrid blends of crumb rubber and metakaolin: Optimization using Response Surface Method. Construction and Building Materials. 2016 Oct 1;123:59-68.

[6] Bing C, Ning L. Experimental research on properties of fresh and hardened rubberised concrete. ASCE J. Mater. Civ. Eng. 2014;26(8):

[7] Naito C, States J, Jackson C, Bewick B. Assessment of crumb rubber concrete for flexural structural members. ASCE J. Mater. Civ. Eng. 2014;26(10)

[8] Eldin NN, Senouci AB. Rubber-tyre particles as concrete aggregate, ASCE J. Mater. Civ. Eng. 1993;5(4):478-496.

[9] Toutanji HA. The use of rubber tyre particles in concrete to replace mineral aggregates. Cement and Concrete Composites 1996;18(2):135-139

[10] Xue J, Shinozuka M. Rubberised concrete: A green structural material with enhanced energy-dissipation capability. Construction and Building Materials 2013;42:196–204

[11] Taha MMR, El-Dieb AS, Ab El-Wahab MA, Abdel-Hameed ME. Mechanical, fracture, and microstructural investigations of rubber concrete. ASCE J. Mater. Civ. Eng. 2008;20(10):640-649

[12] Ganjian E, Khorami M, Maghsoudi AA. Scrap-tyre-rubber replacement for aggregate and filler in concrete. Construction and Building Materials 2009; 23(5):1828–1836

[13] Atahan AO, Yücel AÖ. Crumb rubber in concrete: Static and dynamic evaluation. Construction and Building Materials 2012;36:617–622

[14] He L, Ma Y, Liu Q, Mu Y. Surface modification of crumb rubber and its influence on the mechanical properties of rubber-cement concrete. Construction and Building Materials. 2016 Sep 1;120:403-7.

[15] Fattuhi NI, Clark LA. Cement-based materials containing shredded scrap truck tyre rubber, Construction and Building Materials 1996;10(4): 229-236.

[16] Topçu IB. The properties of rubberised concretes. Cement and Concrete Research 1995;25(2), 304-310.

[17] Turatsinze A, Garros M. On the modulus of elasticity and strain capacity of self-compacting concrete incorporating rubber aggregates. Resources, Conservation and Recycling 2008;52(10): 1209–1215

[18] Aiello MA, Leuzzi F. Waste tyre rubberised concrete: Properties at fresh and hardened state. Waste Management 2010;30(8-9):1696–1704

[19] Cairns RA, Kew HY, Kenny MJ. The use of recycled rubber tyres in concrete construction. In: Sustainable Waste Management and Recycling. Thomas Telford Ltd 2004;135-142 [London, UK]

[20] Khatib ZK, Bayomy FM. Rubberised Portland cement concrete. ASCE J. Mater. Civ. Eng. 1999;11(3): 206-213

[21] Aliabdo AA, Elmoaty AE, AbdElbaset MM. Utilization of waste rubber in non-structural applications. Construction and Building Materials. 2015 Aug 30;91:195-207.

[22] Ghizdăveț Z, Ștefan BM, Nastac D, Vasile O, Bratu M. Sound absorbing materials made by embedding crumb rubber waste in a concrete matrix. Construction and Building Materials. 2016 Oct 15;124:755-63.

[23] Medina NF, Flores-Medina D, Hernández-Olivares F. Influence of fibers partially coated with rubber from tire recycling as aggregate on the acoustical properties of rubberized concrete. Construction and Building Materials. 2016 Dec 30;129:25-36.

[24] Sadek DM, El-Attar MM. Structural behavior of rubberized masonry walls. Journal of Cleaner Production. 2015 Feb 15;89:174-86.

[25] Hall MR, Najim KB. Structural behaviour and durability of steel-reinforced structural Plain/Self-Compacting Rubberised Concrete (PRC/SCRC). Construction and Building Materials. 2014 Dec 30;73:490-7.

[26] Youssf O, ElGawady MA, Mills JE. Experimental investigation of crumb rubber concrete columns under seismic loading. Structures 2015;3:13-27

[27] Ganesan N, Raj B, Shashikala AP. Behavior of Self-Consolidating Rubberized Concrete Beam-Column Joints. ACI Materials Journal. 2013 Nov 1;110(6).

[28] Ismail MK, Hassan AA. Ductility and Cracking Behavior of Reinforced Self-Consolidating Rubberized Concrete Beams. Journal of Materials in Civil Engineering. 2016 Jul 21:04016174.

[29] Ismail MK, Hassan AA. Performance of Full-Scale Self-Consolidating Rubberized Concrete Beams in Flexure. ACI Materials Journal. 2016 Mar 1;113(2).

[30] Elghazouli A.Y., Bompa D.V., Xu B., Stafford P.J., Ruiz-Teran A.M. Inelastic behaviour of RC members incorporating high deformability concrete. fib Symposium 2017 Maastricht, Netherlands

[31] Ghaly AM, Cahill IV JD. Correlation of strength, rubber content, and water to cement ratio in rubberised concrete. Can. J. Civ. Eng. 2005;32(6):1075–1081

[32] Guneyisi E., Gesoglu M, Ozturan T. Properties of rubberised concretes containing silica fume. Cement and Concrete Research 2004;34(12):2309–2317.

[33] AD.RI.A Abruzzo SRL, Adriatica Riciclaggio e Ambiente, Granulato di Gomma, http://www.adria-abruzzo.it/ADRIA/index.html

[34] CONICA, Recycled Rubber from Used Tyres, http://www.conica.com/en/commodities/black-granules/rubber-granules/recycled-tyre-rubber/

[35] Anagennisi Project, 'Innovative Use of all Tyre Components in Concrete': h*ttp://www.anagennisi.org/*

[36] Pilakoutas K, Raffoul S, Papastergiou P, Garcia R, Guadagnini M, Hajirasouliha I, A study of the reuse of all tyre components in concrete; The Anagennisi Project. Int. Conference on Sustainable Structural Concrete, 15-18 Sept 2015, La Plata, Argentina; 259-268, paper 221

[37] Raffoul S, Garcia R, Pilakoutas K, Guadagnini M, Hajirasouliha I, Fresh properties and stress-strain behaviour of crumb rubberised concrete in axial compression. Int. Conference on Sustainable Structural Concrete, 15-18 Sept 2015, La Plata, Argentina; 269-277, paper 222.

[38] Raffoul S, Garcia R, Pilakoutas K, Guadagnini M, Flores Medina N, Optimisation of rubberised concrete with high rubber content: An experimental investigation; Construction and Building Materials 2016; 124:391-404.

[39] TARMAC, Tarmac Trupak building aggregates, http://www.tarmac.com/building-aggregates/

[40] CEN (European Committee for Standardization) EN 933-1:2012 Tests for geometrical properties of aggregates - Part 1: Determination of particle size distribution - Sieving method. CEN, Brussels (Belgium); 2012

[41] HOPE Construction Materials, High Strength 52.5N Cement, http://hopecement.com/product/high-strength-52-5n-cement/

[42] Sika ViscoFlow 1000, High range water reducing/superplasticing concrete admixture with enhanced workability retention, Product data sheet, Edition 21/5/2015, Sika Limited, UK.

[43] Sika ViscoFlow 2000, High range water reducing/superplasticing concrete admixture with enhanced workability retention, Product data sheet, Edition 17/2/2016, Sika Limited, UK.

[44] CEN (European Committee for Standardization) EN 450-1:2012 Fly ash for concrete - Part 1: Definition, specifications and conformity criteria. CEN, Brussels (Belgium);; 2012

[45] ELKEM, Elkem Microsilica Grade 940 for Concrete, https://www.elkem.com/silicon-materials/high-performance-concrete/microsilica-concrete-grades/microsilica-grade-940-construction/

[46] CEN (European Committee for Standardization) (EN 206-1:2000 Concrete — Part 1: Specification, performance, production and conformity. CEN, Brussels (Belgium); 2000

[47] ASTM International. C39/C39M − 15 Standard Test Method for Compressive Strength of Cylindrical Concrete Specimens, West Conshohocken (USA); 2015

[48] RILEM Technical Committees. RILEM TC 148-SSC: Strain Softening of Concrete-test Methods for Compressive Softening. Mat. Struct. 2000;33(6):347-351

[49] van Mier JGM, Shah SP, Arnaud M et al. Strain-softening of concrete in uniaxial compression. Mat. Struct. 1997;30(4):195-209

[50] ASTM International. C496/C496M − 11 Standard Test Method for Splitting Tensile Strength of Cylindrical Concrete Specimens, West Conshohocken (USA); 2011

[51] Su H, Yang J, Ling TC, Ghataora GS, Dirar S. Properties of concrete prepared with waste tyre rubber particles of uniform and varying sizes. Journal of Cleaner Production 2015;91:288-296

[52] Azevedo F, Pacheco-Torgal F, Jesus C, Barroso de Aguiar JL, Camões AF. Properties and durability of HPC with tyre rubber wastes. Construction and Building Materials 2012; 34:186–191

[53] Bignozzi MC, Sandrolini F. Tyre rubber waste recycling in self-compacting concrete. Cement and Concrete Research 2006;36(4):735–739

[54] Liu F, Zheng W, Li L, Feng W, Ning F. Mechanical and fatigue performance of rubber concrete. Construction and Building Materials 2013;47:711–719

[55] Atahan AO, Sevim UK. Testing and comparison of concrete barriers containing shredded waste tire chips, Materials Letters (2008);62(21-22):3754–3757

[56] Zheng L, Huo XS,Yuan Y. Strength, modulus of elasticity, and brittleness index of rubberised concrete. ASCE J. Mater. Civ. Eng. 2008;20(11): 692-699

[57] Neville AM. Properties of concrete, 4th Ed., Longman, London (UK); 1993

[58] Mansur, M. and Islam, M. Interpretation of concrete strength for nonstandard specimens. ASCE J. Mater. Civ. Eng. 2002;14(2):151-155.

[59] Yi ST, Yang IK, Choi JC. Effect of specimen sizes, specimen shapes, and placement directions on compressive strength of concrete. Nuclear Engineering and Design 2006;23(2):115–127

[60] Nielsen MP and Hoang LC. Limit analysis and concrete plasticity, Third edition. 816 Pages, CRC Press, Taylor and Francis Group, Boca Raton (FL, USA); 2010

[61] Neville AM. The relation between standard deviation and mean strength of concrete test cubes. Magazine of Concrete Research 1959;11(32):75-84

[62] Himsworth FR. The variability of concrete and its effect on mix design. Proceedings of the Institution of Civil Engineers 1945;3(2):163-200

[63] CEN (European Committee for Standardization). EN 1992-1-1, Eurocode 2: Design of concrete structures, Part 1–1: General rules for buildings. CEN, Brussels (Belgium); 2004

[64] fib Model Code 2010. fib bulletins 65 and 66. fib, Lausanne (Switzerland); 2012

[65] Reinhardt H, Cornelissen H, Hordijk D. Tensile Tests and Failure Analysis of Concrete. J. Struct. Eng. 1986;112(11):2462-2477.

[66] Najim KB, Hall MR. Crumb rubber aggregate coatings/pre-treatments and their effects on interfacial bonding, air entrapment and fracture toughness in self-compacting rubberised concrete (SCRC), Mater Struct 2013;46(12):2029-2043

[67] Hordijk DA. Tensile and tensile fatigue behaviour of concrete; experiments, modelling and analyses. Heron. 1992;37(1).

List of figures

List of tables

Nomenclature

Greek letters

σ - *stress*

$\varepsilon_{c01,1}$ – crushing strain for normal concrete

ε_{cr1} - axial strain

$\varepsilon_{cr1,1}$ – crushing strain for rubberised concrete

ε_{cr2} – lateral strain

$\varepsilon_{cr1,u}$ – ultimate strain of rubberised concrete at complete loss of strength

$\varepsilon_{cr1(\eta fcr)}$ – *axial strain at* $\eta \times f_{cr}$

$\varepsilon_{cr2(\eta fcr)}$ – *lateral strain at* $\eta \times f_{cr}$

$\varepsilon_{cr1,el}$ strain at proportionality limit

η – stress factor

λ – factor for the type of aggregate replaced

ρ_{vr} – volumetric rubber ratio

Lowercase latin letters

$d_{g,repl}$ – replaced aggregate size

$d_{g,max}$ – maximum mineral aggregate size

$d_{r,avg}$ – average rubber particle size

$d_{r,max}$ maximum rubber particle size

f_{c0} – normal concrete cylinder compressive strength

f_{cr} – rubberised concrete cylinder compressive strength

$f_{cr,cube}$ – rubberised concrete cube compressive strength

f_{ctr} – rubberised concrete tensile strength

$f_{ctr,sp}$ - rubberised concrete splitting strength

$f_{cr,ref}$ mechanical strength of the reference sample

$f_{cr(d)}$ converted mechanical strength of the sample

$g_{c,2}$ – post-crushing energy

$w_{max,r}$ – maximum crack displacement

w_{max0} – base crack displacement

Uppercase latin letters

G_c – crushing energy

E_{cr} – elastic modulus

$V_{cr,ref}$ - volume of the reference sample

$V_{cr(d)}$ - converted volume of the sample

Tables

Table 1 Results of the pilot tests

Sample	f_{cr} (MPa)	$\varepsilon_{cr1,1}$ (mm/mm)	E_{cr} (MPa)	G_c (N/mm)
R60-00	5.97	0.00165	4208	9.8
R60-0P	6.43	0.00148	6351	10.9
R60-JP	6.62	0.00208	3855	10.2
R60-J0	6.52	0.00176	4305	10.2
dev.	± 0.28	± 0.000253	± 1130	± 0.45

Table 2 Summary of test results

ρ_{vr} (-)	f_{cr} (MPa)	$f_{cr,cube}$ (MPa)	$f_{ctr,sp}$ (MPa)	$\varepsilon_{cr1,1}$ (mm/mm)	$\varepsilon_{cr2,1}$ (mm/mm)	E_{cr} (MPa)	G_c (N/mm)
0	70.2	77.0	4.99	0.002277	-0.00115	42302	9.13
0.20	29.7	50.7	3.12	0.002130	-0.00120	19608	7.63
0.40	13.3	24.6	1.98	0.001373	-0.00128	14124	9.86
0.60	7.06	11.8	1.20	0.001366	-0.00130	9028	10.5

Table 3 Predictions of Equation (2)

Author	n_{mixes} (-)	$f_{c,0}$ (MPa)	$\rho_{vr,min}$ (-)	$\rho_{vr,max}$ (-)	$d_{r,max}$ (mm)	$d_{g,max}$ (mm)	$f_{cr,test}/f_{cr,pred}$ (-) Average	COV
This paper	3	70.2	0.200	0.600	14	10	1.04	0.08
Guneyisi et al. (2004) [32]	60	61.2-87.9	0.025	0.500	40	20	1.05	0.08
Hernandez et al (2002) [1]	4	97.2	0.030	0.080	22	20	0.88	0.09
Khatib and Bayomy (1999) [20]	8	39.6	0.025	0.500	50	20	0.78	0.17
Naito et al (2014) [7]	3	46.8	0.100	0.300	9.5	12	1.31	0.13
Su et al. (2015) [51]	4	61.1	0.072	0.082	5.0	20	1.26	0.03
Xue and Shinozuka (2013) [10]	8	38.2	0.032	0.128	6.0	12	0.91	0.11
TOTAL (CA+FA)	90						1.03	0.10

Author	n_{mixes} (-)	$f_{c,0}$ (MPa)	$\rho_{vr,min}$ (-)	$\rho_{vr,max}$ (-)	$d_{r,max}$ (mm)	$d_{g,max}$ (mm)	$f_{cr,test}/f_{cr,pred}$ (-) Average	COV
Aiello and Leuzzi (2009) [18]	4	27.8	0.023	0.112	20	18	0.91	0.04
Azevedo et al. (2012) [52]	9	71.1	0.028	0.153	4.8	9.5	0.80	0.21
Bignozzi and Sandrolini (2006) [53]	2	33.9	0.137	0.205	2.0	20	1.30	0.06
Cairns et al. (2004) [19]	3	51.3	0.050	0.250	5.0	10	1.13	0.22
Eldin and Senouci (1993) [8]	4	35.3	0.090	0.360	6.0	19	1.17	0.17
Ghaly and Cahill (2005) [31]	9	12.7-27.7	0.081	0.256	2.0	20	1.05	0.07
Khatib and Bayomy (1999) [20]	8	39.6	0.022	0.434	5.0	20	0.76	0.30
Liu et al. (2013) [54]	3	44.5	0.015	0.045	2.0	12	0.80	0.13
Raffoul et al. (2016) [38]	5	63.3	0.045	0.600	20	20	0.97	0.07
Taha et al (2008) [11]	4	27.4	0.176	0.352	20	20	1.30	0.09
Topcu (1995) [16]	3	35.3	0.052	0.156	1.0	18	0.79	0.10
TOTAL (FA)	54						1.00	0.13

Author	n_{mixes} (-)	$f_{c,0}$ (MPa)	$\rho_{vr,min}$ (-)	$\rho_{vr,max}$ (-)	$d_{r,max}$ (mm)	$d_{g,max}$ (mm)	$f_{cr,test}/f_{cr,pred}$ (-) Average	COV
Aiello and Leuzzi (2009) [18]	3	47.0	0.062	0.188	20	20	0.67	0.08
Atahan and Sevim (2008) [55]	5	38.2	0.045	0.222	-	-	0.77	0.11
Bing and Ning (2014) [6]	8	37.6-63.5	0.156	0.622	20	20	1.40	0.14
Cairns et al. (2004) [19]	3	51.3	0.050	0.250	5.0	10	1.06	0.13
Eldin and Senouci (1993) [8]	4	34.9	0.160	0.640	38	25	1.10	0.12
Ganjian et al. (2009) [12]	3	33.9	0.024	0.049	25	16	0.95	0.09
Khatib and Bayomy (1999) [20]	8	39.6	0.028	0.566	50	20	0.50	0.20
Naito et al (2014) [7]	2	46.8	0.133	0.267	10	40	1.06	0.14
Taha et al (2008) [11]	4	27.4	0.088	0.648	20	20	1.34	0.16
Topcu (1995) [16]	3	35.3	0.098	0.294	4.0	10	0.74	0.13
Toutanji (1996) [9]	4	32.0	0.150	0.600	13	16	1.25	0.15
Turatsinze and Garros (2008) [17]	4	44.1	0.102	0.254	10	19	0.76	0.15
Zheng et al (2008) [56]	3	56.0	0.096	0.289	32	20	1.27	0.09
TOTAL (CA)	54						0.99	0.13

Figures

a)

b)

Figure 1 a) Rubberised concrete constituents b) Rubberised concrete mix

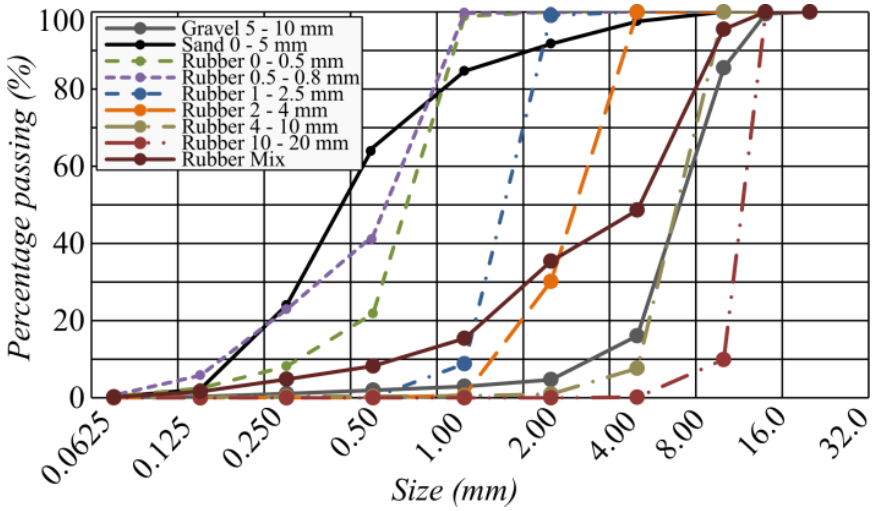

Figure 2 Sieve analysis for mineral aggregates and waste rubber

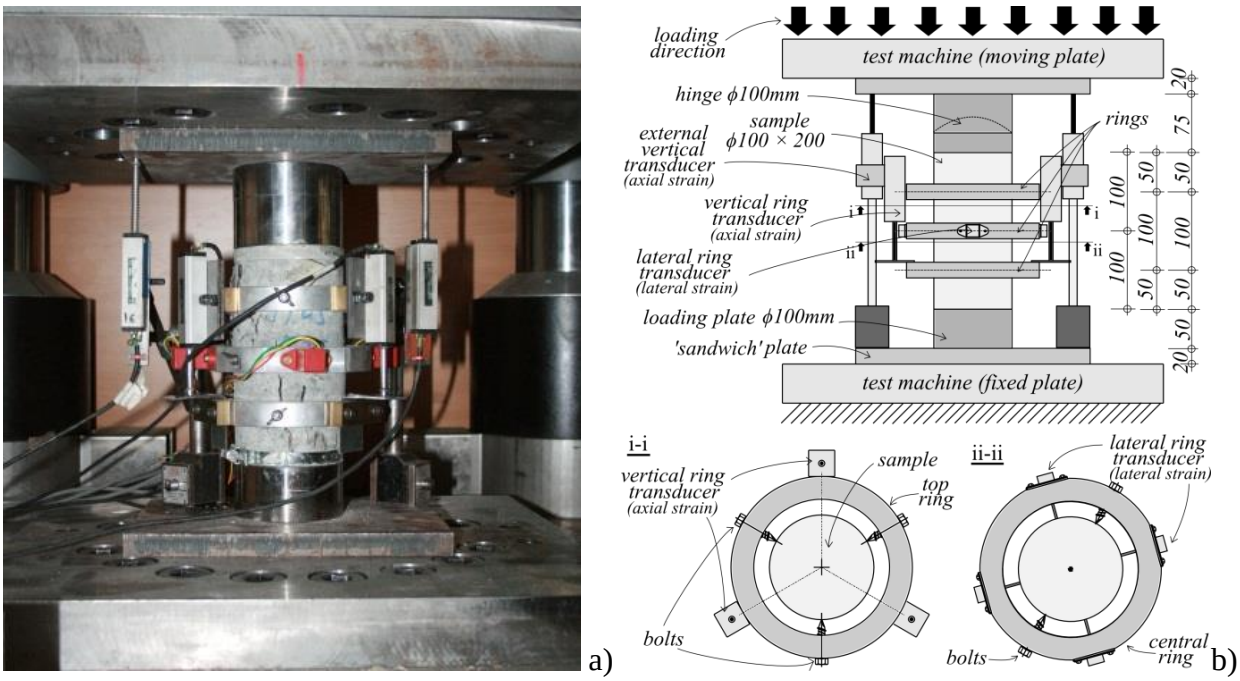

Figure 3 Testing arrangement for cylinders a) general view, b) layout

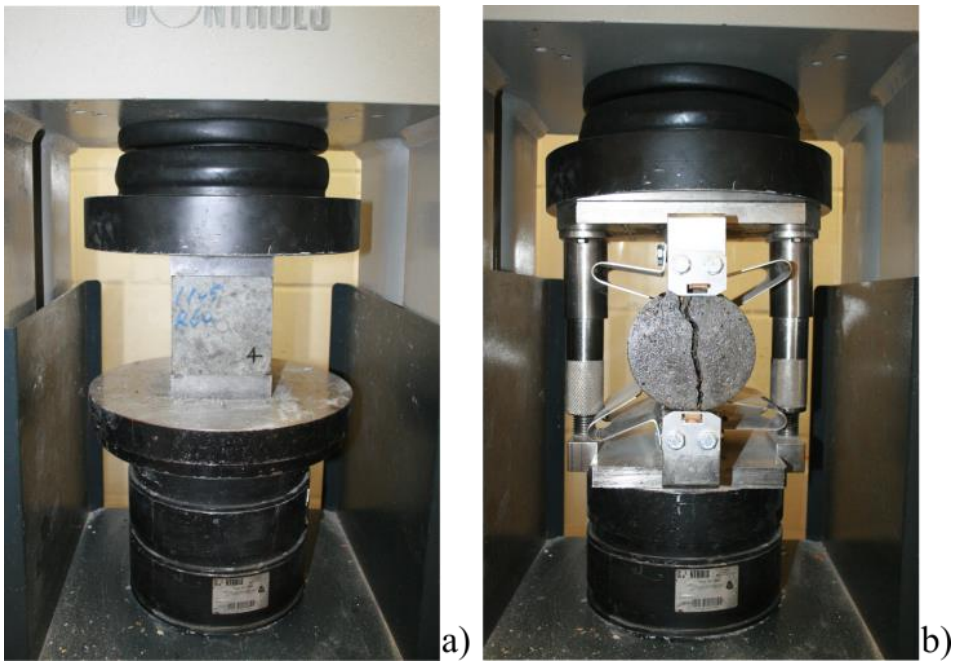

Figure 4 View of testing for: a) compression test on cubes, b) splitting test on cylinders

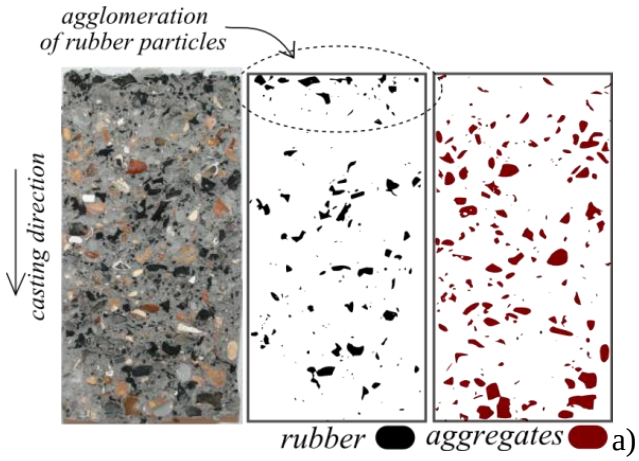

a)

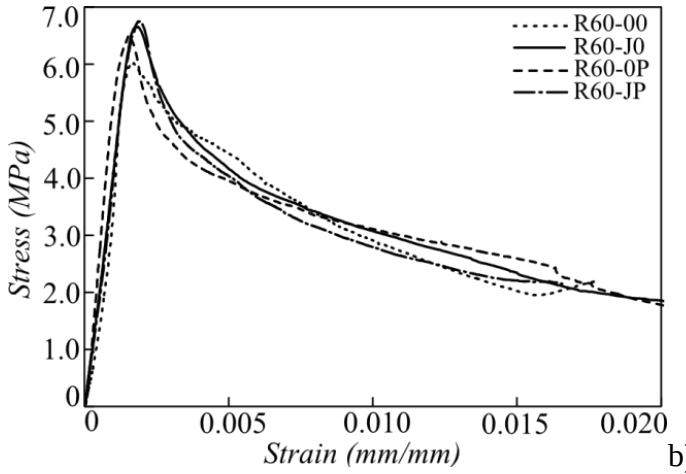

b)

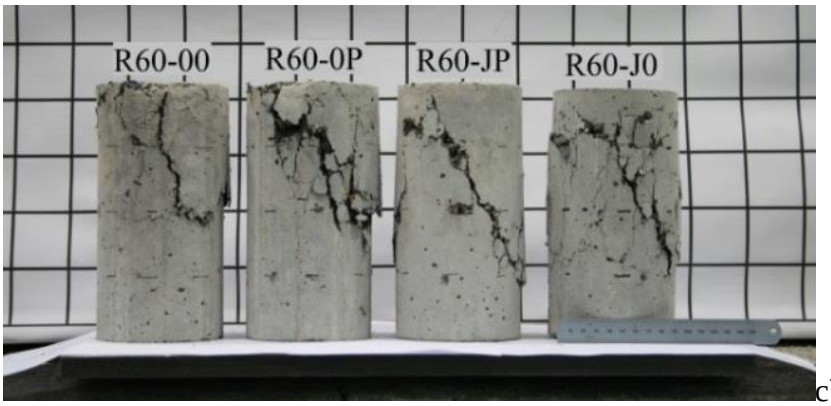

c)

Figure 5 a) Longitudinal cross section through a rubberised concrete cylinder b) Stress – strain response of pilot tests with 60% replacement, c) Failure of pilot cylindrical samples

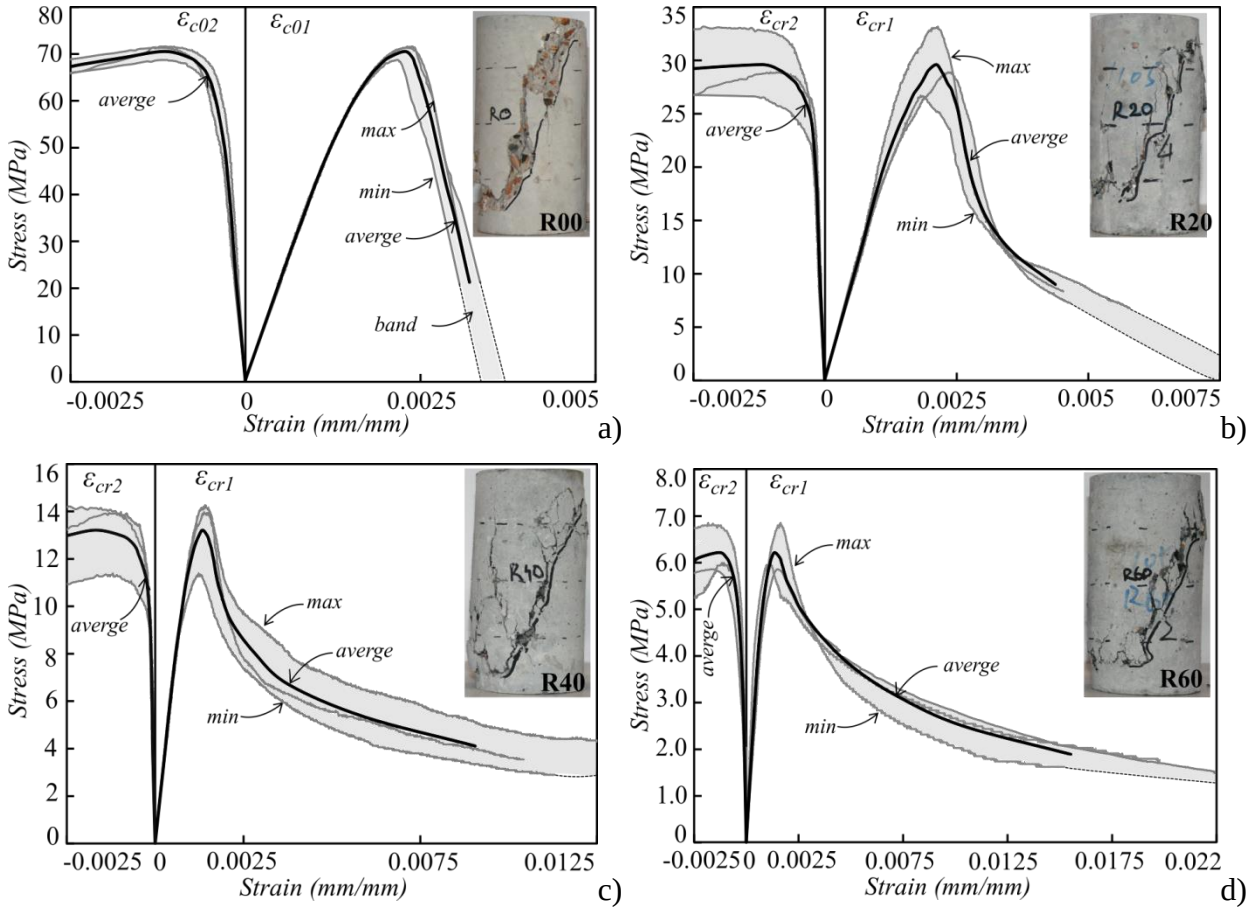

Figure 6 Stress-strain relationships for a) normal concrete R00, b) rubberised concrete with 20% replacement R20, c) rubberised concrete with 40% replacement R40, d) rubberised concrete with 60% replacement R60.

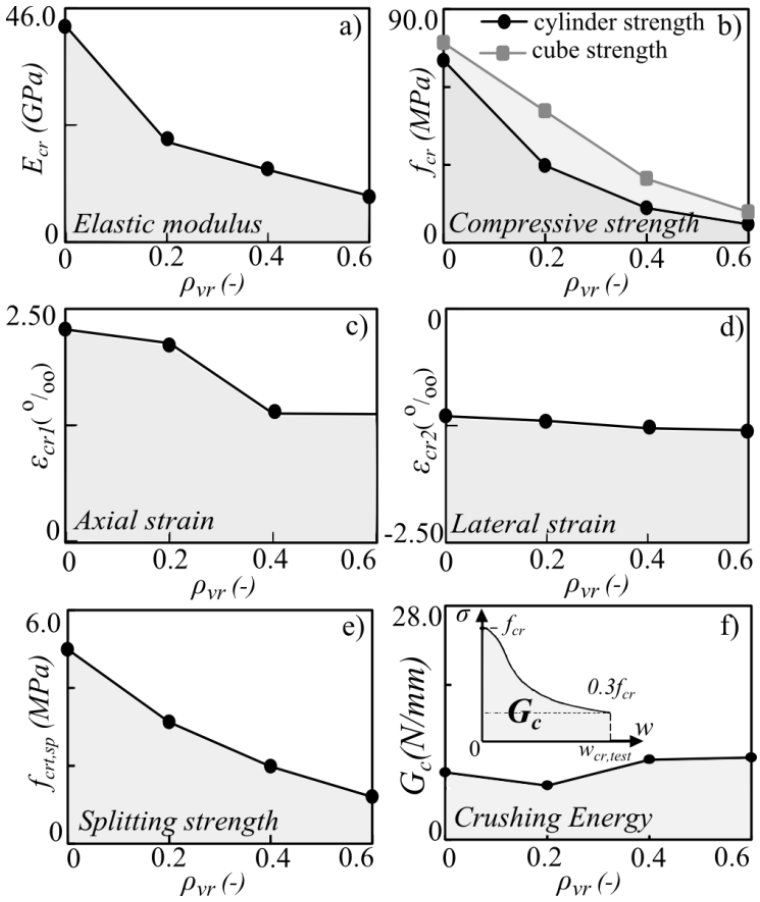

Figure 7 Influence of rubber content ρ_{vr} to the mechanical properties of concrete a) elastic modulus E_{cr}, b) compressive strength f_{cr}, c) peak axial strain $\varepsilon_{cr1,1}$, d) peak lateral strain $\varepsilon_{cr2,1}$, e) splitting strength $f_{ctr,sp}$ f) crushing energy G_c

Figure 8 Comparative overview of test samples

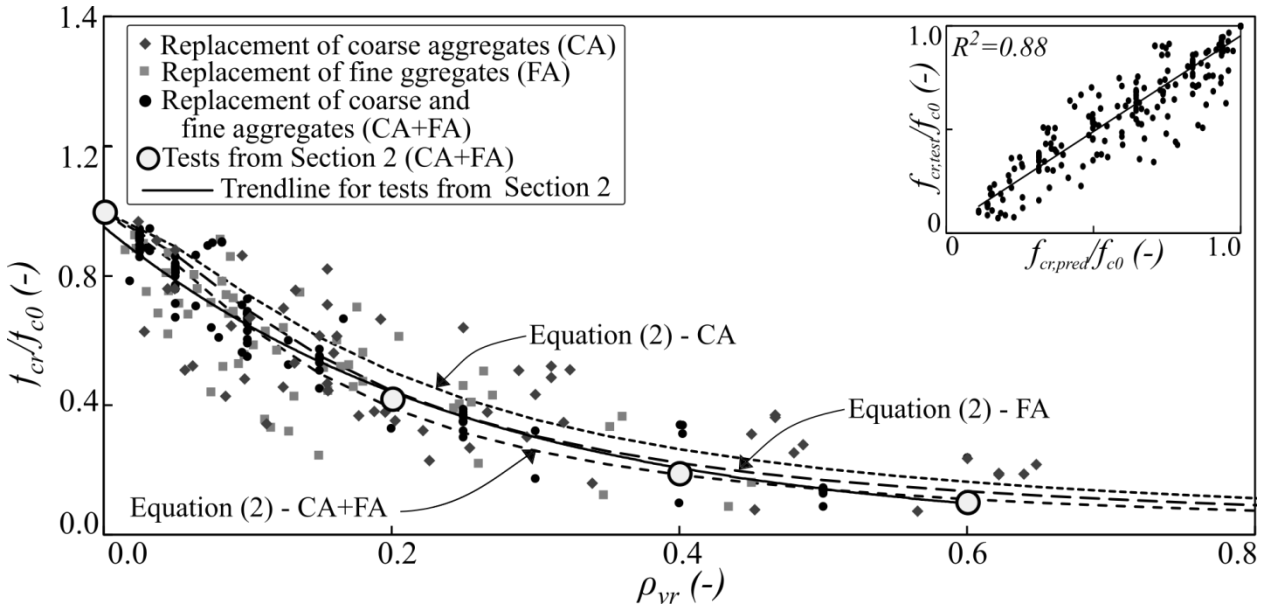

Figure 9 Compressive strength degradation as a function of volumetric rubber ratio ρ_{vr}

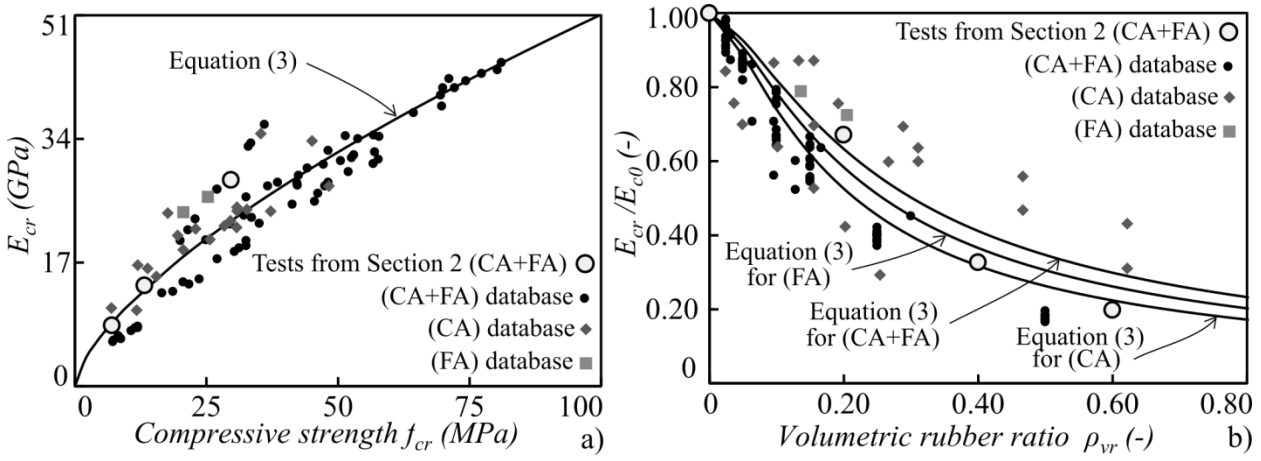

Figure 10 a) relationship between modulus of elasticity E_{cr} and compressive strength f_{cr} for rubberised concrete, b) degradation of stiffness as a function of volumetric rubber ratio ρ_{vr}

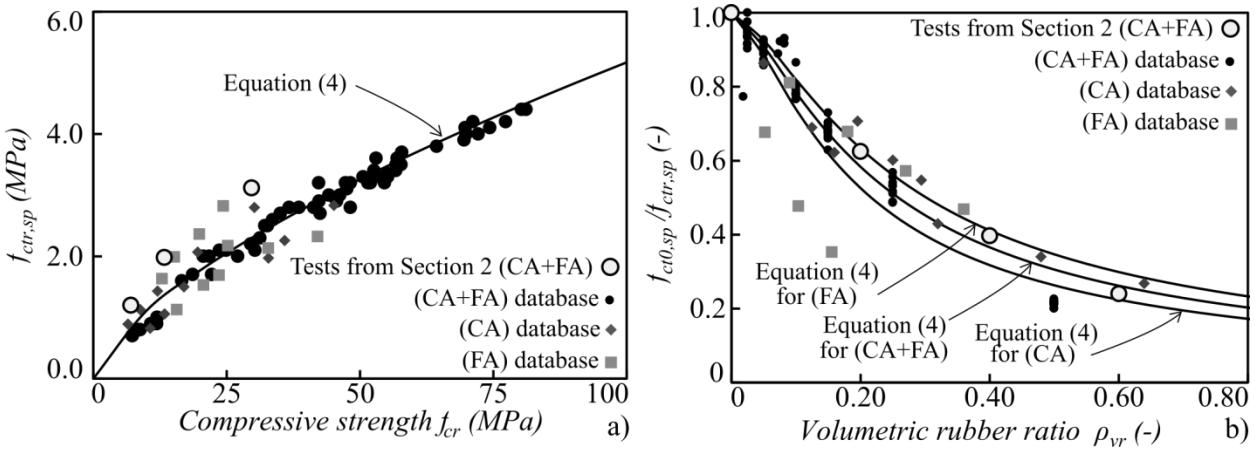

Figure 11 a) relationship between splitting strength $f_{ctr,sp}$ and compressive strength f_{cr} for rubberised concrete, b) degradation of $f_{ctr,sp}$ as a function of volumetric rubber ratio ρ_{vr}

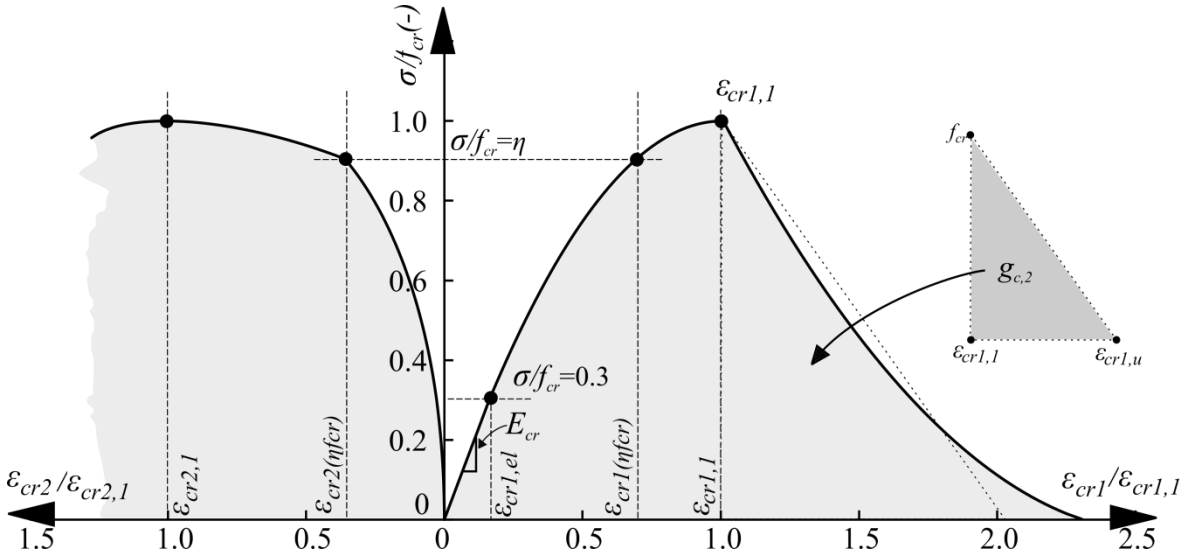

Figure 12 Uniaxial constitutive model for rubberised concrete

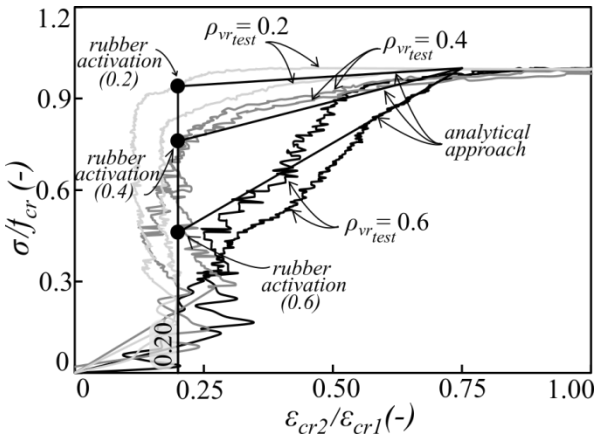

Figure 13 Relationship between stress ratio and lateral-to-axial strain ratio

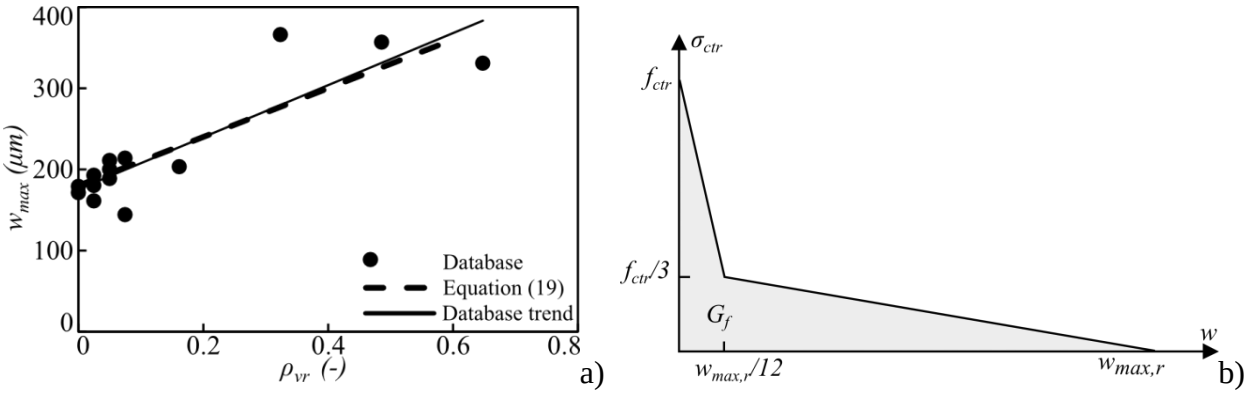

Figure 14 a) relationship between maximum crack width and rubber content, b) assumed stress-strain diagram in tension

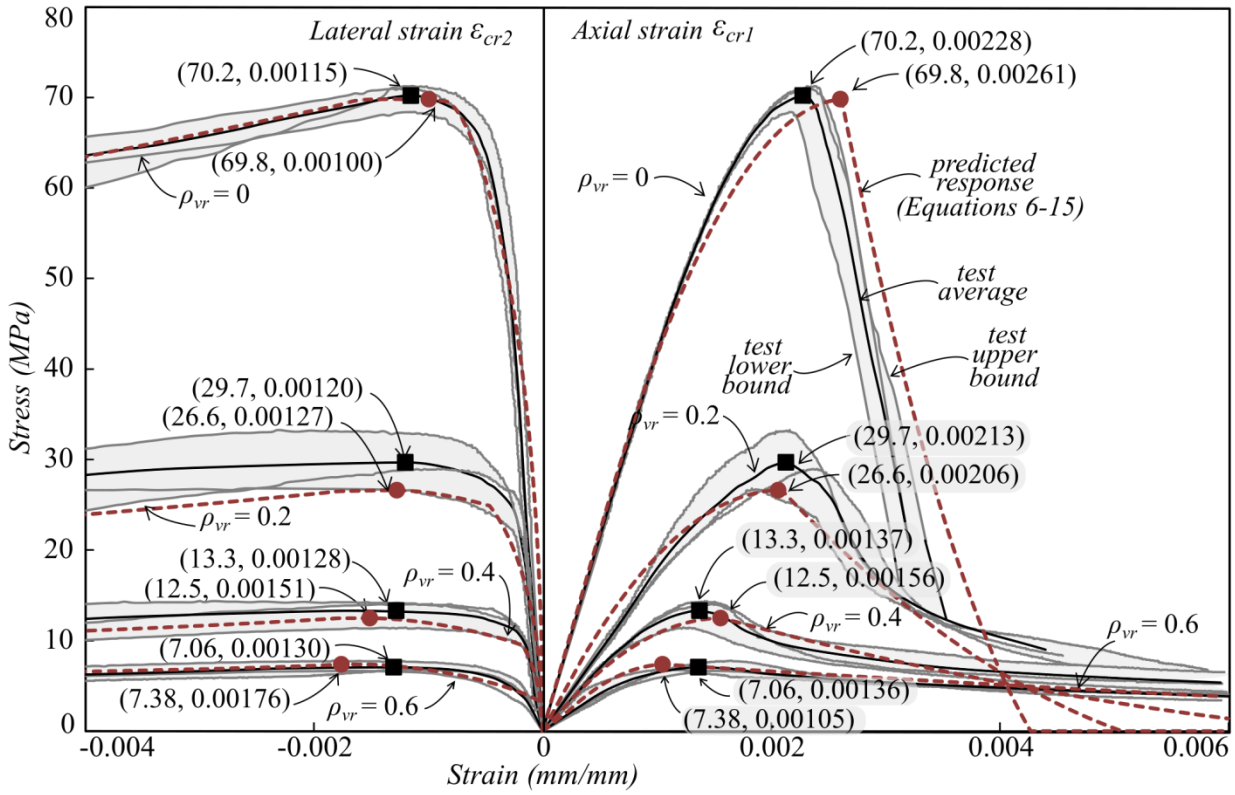

Figure 15 Comparative assessment between test and predicted stress-strain responses (black and red curves represent experimental and predicted response, respectively)

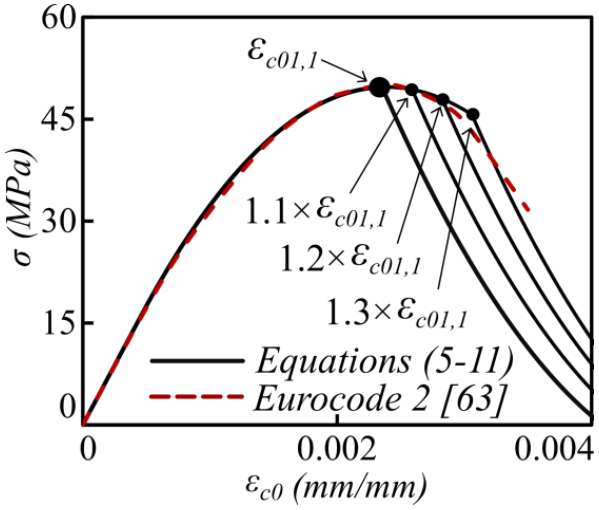

Figure 16 Comparative assessments between stress-strain responses predicted by Eurocode 2 [63] and the proposed model